Acta Cryst. (1996). B**52**, 260–265

Structure and Optical Non-linearity of $PbO.2B_2O_3$

D. L. Corker and A. M. Glazer

Department of Physics, Clarendon Laboratory, University of Oxford, Parks Road, Oxford OX1 3PU, England

(*Received 13 July 1995; accepted 27 September 1995*)

Abstract

The crystal structure of lead tetraborate, $PbO.2B_2O_3$, has been refined using single-crystal X-ray diffraction data (Mo $K\alpha$ radiation, $\lambda = 0.71069$ Å). Crystal data at room temperature: $M_r = 362.43$, orthorhombic, $P2_1nm$ (C_{2v}^7), $a = 4.251(2)$, $b = 4.463(3)$, $c = 10.860(3)$ Å, $V = 206.04$ Å^3 with $Z = 2$, $\mu = 402.6$ cm^{-1}, $D_x = 5.88$ Mg m^{-3}, $F(000) = 316$, final $R = 0.022$, $wR = 0.025$ over 655 reflections with $I > 2.5\sigma(I)$. Atomic coordinates are in general agreement with those previously reported for the isostructural compound, $SrO.2B_2O_3$, by Perloff & Block [*Acta Cryst.* (1966), **20**, 274–279]. All the borons are tetrahedrally coordinated with a three-dimensional network formed from O atoms that are common to either two or three tetrahedra. The tetrahedra show deformation because the B—O bonds involving the two-coordinated O atoms are much shorter than those involved with three-coordinated O atoms. The Pb atoms are situated in empty tunnels running along [010] left by the network of tetrahedra. The Pb atoms display a highly asymmetric distribution of Pb—O bonding, with the five shortest bonds covering the range 2.483(5)–2.664(5) Å, being all situated to one side of the Pb atom. Preliminary investigations of the non-linear optical behaviour of lead tetraborate are also discussed. The results indicate that doping with barium should lead to a new non-linear optical material that is both phase-matchable and has a high optical non-linearity.

1. Introduction

Since the discovery of BBO [β-$Ba_3(B_3O_6)_2$] and LBO (LiB_3O_5) at the Fujian Institute of Research in China (Chen, Wu & Li, 1989), many researchers have become interested in borate crystals as potential non-linear optical (NLO) materials for use in frequency conversion of lasers. As part of our search for new NLO materials, we selected lead tetraborate for investigation primarily because of the highly asymmetric bonding reported in SrB_4O_7 and also because of the unusual type of borate framework present: the B atom is tetrahedrally coordinated with three tetrahedra sharing one common oxygen. The advantage of highly asymmetric bonding in a structure is most easily described by considering the Bond Polarizability theory (Jeggo, 1971). According to this theory the non-linear behaviour of a material is reduced to a sum of contributions from all the chemical bonds within the structure. The contribution of a particular bond of specific length to the overall non-linearity tensor is given by a term called the NLO bond polarizability 'β'. As a first approximation the components of the NLO bond polarizability perpendicular to a bond can be considered to be negligible compared with the component parallel to the bond. Addition of each bond contribution tensorially leads to the term

$$\Delta_{ijk} = (1/V)\Sigma_b \alpha_i^{(b)} \alpha_j^{(b)} \alpha_k^{(b)} \beta^{(b)}, \quad (1)$$

where $\beta^{(b)}$ is the NLO polarizability running along bond b, $\alpha_i^{(b)}$, $\alpha_j^{(b)}$ and $\alpha_k^{(b)}$ are the direction cosines of bond b relative to the crystal axes and V is the unit-cell volume. The term Δ_{ijk} is a quantity, called the Miller tensor (Miller, 1964), which can be directly related to the **d** tensor, commonly used to represent a material's frequency doubling capability and more generally the material's optical non-linearity, such that

$$d_{ijk} = \Delta_{ijk} \chi_i^{(2\omega)} \chi_j^{(\omega)} \chi_k^{(\omega)}, \quad (2)$$

where $\chi_i^{(2\omega)}$ is the linear susceptibility at the doubled frequency and $\chi_j^{(\omega)}$ and $\chi_k^{(\omega)}$ are the appropriate linear susceptibilities at the fundamental frequency.

Without even considering the magnitudes of the NLO bond polarizabilities, it is possible to see why highly symmetrical bonding, such as that found in undistorted octahedra, would lead to greater cancellation in (1) and hence a low optical non-linearity and frequency doubling efficiency. Similarly, highly asymmetric bonding, where the majority of highly polarizable electron density lies to one side of a central atom, leads to significantly less cancellation in this term and hence a greater non-linearity.

In this paper we describe a precise refinement of the crystal structure of lead tetraborate. The isostructural strontium tetraborate structural determination had originally been reported by Perloff & Block (1966). In addition to the structural details of lead tetraborate, we give the results of measurements of the second-harmonic generation (SHG) efficiency of powdered samples, showing that lead tetraborate has an SHG efficiency of approximately 8–16 times greater than

ISSN 0108-7681

KDP (KH_2PO_4). However, when the SHG efficiency is estimated in samples of varying particle sizes, lead tetraborate exhibits the characteristics of a non-phase-matchable* (NPM) material. This implies that this estimate of non-linearity is likely to be much lower than the true value. Further support for the higher optical non-linearity of lead tetraborate arises from samples doped with barium. In these samples phase-matchability and an SHG efficiency several times greater is indicated.

2. Synthesis

Crystals of lead tetraborate were grown from a stoichiometric melt of PbO and B_2O_3. Both powders were ground together and sealed in a platinum crucible, which was then heated to 1058 K, held for 12 h and cooled down at 8 K h^{-1}. Transparent colourless crystals which grew during cooling were generally in the size range 0.02–0.1 mm and showed sharp extinction under the polarizing microscope. The crystals were then washed with water to remove any attached flux. The crystals were identified as lead tetraborate by taking a small sample of crystals and grinding them into a powder. This powder was then identified from its X-ray diffraction pattern. The highest 30 peaks were used in the automatic indexing program *INDEX* (Stoe & Cie, 1985) to give the cell parameters a = 4.243, b = 4.455 and c = 10.840 Å with a figure of merit of 19.9, in full agreement with those reported by Perloff & Block (1966).

3. Data collection

A single crystal of dimensions 0.04 × 0.05 × 0.06 mm was selected for data collection on a Stoe Stadi-4 single-crystal diffractometer using Mo $K\alpha$ radiation (λ = 0.71069 Å) and the ω–2θ scan mode at room temperature. The primitive orthorhombic unit cell constants were found by collecting 25 reflections. These were refined using least-squares methods to the values a = 4.263 (2), b = 4.475 (2) and c = 10.884 (5) Å. Data were then collected over the 2θ range 3–65°, giving a total of 2088 reflections with $-6 < h < 6$, $0 < k < 6$ and $0 < l < 16$. During data collection, three standard reflections 020, 200 and 114 were monitored every hour and a crystal orientation check was taken after every three standards. Cell constants were then refined using nine high-2θ reflections extracted from the data collection and measured with double step-scans to give the final cell parameters a = 4.251 (2), b = 4.463 (3) and c = 10.860 (3) Å. Data reduction was performed using the program *REDU*4 (Stoe & Cie, 1985) to give a total of 788 merged reflections. The observed systematic absences, $h0l$, $h + l = 2n + 1$; $h00$, $h = 2n + 1$; and $00l$, $l = 2n + 1$, combined with the knowledge that the material exhibited second-harmonic generation and was therefore non-centrosymmetric, allowed only the space group $P2_1nm$. The collected data were corrected for absorption using a combination of spherical absorption (R = 0.025 mm, μR = 0.95) and ψ-scan data (T_{min} = 0.1568, T_{max} = 0.2388). The initial model was based on that of strontium tetraborate, $SrO.2B_2O_3$, reported by Perloff & Block (1966). Reflections with $I < 2.5\sigma(I)$ were removed from the refinement and anomalous dispersion was allowed for. The function minimized was $\Sigma w(|F_o| - |F_c|)^2$, where the weights were calculated using a robust/resistant weighting scheme (Prince, 1982).

Refinement of positional and thermal parameters proceeded without problems using the program *CRYSTALS* (Watkin, Carruthers & Betteridge, 1985), to a final R factor of 0.022. This was performed with the lighter atoms B and O refined isotropically and the heavier Pb atom anisotropically. The refinement was concluded when all shifts were at least one order of magnitude smaller than the standard deviations in both thermal and positional parameters. Experimental details are summarized in Table 1. The final atomic and thermal parameters for lead tetraborate are given in Table 2, while the associated bond distances are given in Table 3.* For comparison Table 3 also quotes the Sr—O bond distances in $SrO.2B_2O_3$, given by Perloff & Block (1966).

4. Structure

The structure of lead tetraborate consists of a three-dimensional borate network which may be considered either as consisting of B_3O_9 six-membered rings or, as all borons are tetrahedrally coordinated, the network may be considered simply as corner-linked tetrahedra.

The six-membered rings join each other to form chains along the [100] direction, which then link *via* O atoms in the [010] and [001] directions. The most prominent and extremely unusual feature of the structure

* For a non-linear material to be an efficient second-harmonic generator, it must possess the ability to be phase-matched. Phase-matching is a technique whereby the birefringence of a crystal is used to counteract the devastating effect of dispersion on the transfer of energy from the fundamental wave to the second-harmonic wave (Hobden, 1967). This is usually achieved by using two different types of waves for the fundamental and second-harmonic beams. For example, in the case of a negative uniaxial crystal, phase-matching could be achieved by sending the fundamental into the crystal as an ordinary wave, while the second harmonic could be generated as an extraordinary wave propagating at θ_{pm} such that $n_e^{2\omega}(\theta_{pm}) = n_o^{\omega}$. From this equality it can be seen that phase-matchability can only be achieved in materials which possess sufficient birefringence to offset the dispersion.

* Lists of structure factors and anisotropic displacement parameters have been deposited with the IUCr (Reference: BM0004). Copies may be obtained through The Managing Editor, International Union of Crystallography, 5 Abbey Square, Chester CH1 2HU, England.

Table 1. *Experimental details*

Crystal data	
Chemical formula	$PbO.2B_2O_3$
Chemical formula weight	362.43
Cell setting	Orthorhombic
Space group	$P2_1nm$
a (Å)	4.251 (2)
b (Å)	4.463 (3)
c (Å)	10.860 (3)
V (Å^3)	206.04
Z	2
D_x (Mg m^{-3})	5.88
Radiation type	Mo $K\alpha$
Wavelength (Å)	0.71069
No. of reflections for cell parameters	9
θ range (°)	25–30
μ (mm^{-1})	40.26
Temperature (K)	293
Crystal form	Irregular
Crystal size (mm)	0.06 × 0.05 × 0.04
Crystal colour	Colourless
Data collection	
Diffractometer	Stoe Stadi-4
Data collection method	ω–2θ
Absorption correction	Spherical and ψ scans
T_{min}	0.1568
T_{max}	0.2388
No. of measured reflections	2088
No. of independent reflections	788
No. of observed reflections	655
Criterion for observed reflections	$I > 2.5\sigma(I)$
R_{int}	0.0535
θ_{max} (°)	32.5
Range of h, k, l	$-6 \rightarrow h \rightarrow 6$ $0 \rightarrow k \rightarrow 6$ $0 \rightarrow l \rightarrow 16$
No. of standard reflections	3
Frequency of standard reflections	60
Intensity decay (%)	3
Refinement	
Refinement on	F
R	0.0223
wR	0.0252
S	1.07
No. of reflections used in refinement	655
No. of parameters used	32
Weighting scheme	Tukey & Prince (Prince, 1982), three parameters (3.47, −3.39, 1.99)
$(\Delta/\sigma)_{max}$	0.0001
$\Delta\rho_{max}$ (e Å^{-3})	2.1
$\Delta\rho_{min}$ (e Å^{-3})	−1.8
Extinction method	Larson (1970)
Extinction coefficient	2.1 (4)
Source of atomic scattering factors	*International Tables for X-ray Crystallography* (1974, Vol. IV)

Table 2. *Fractional atomic coordinates and equivalent isotropic displacement parameters (Å^2)*

	Occupancy	x	y	z	U_{iso}
Pb(1)	1.0	−0.0318 (2)	0.19835 (8)	0.0	0.0067 (7)†
O(1)	1.0	0.584 (2)	0.765 (2)	0.0	0.004 (1)
O(2)	1.0	0.550 (1)	0.362 (1)	0.1448 (5)	0.0052 (9)
O(3)	1.0	0.143 (1)	0.730 (1)	−0.1361 (5)	0.0045 (8)
O(4)	1.0	0.150 (1)	0.128 (1)	0.2805 (5)	0.0040 (8)
B(1)	1.0	−0.025 (4)	0.325 (1)	0.3776 (5)	0.0029 (8)
B(2)	1.0	0.003 (2)	0.820 (2)	0.2479 (5)	0.004 (1)

† $U_{eq} = (1/3)\Sigma_i\Sigma_j U_{ij} a_i^* a_j^* \mathbf{a}_i.\mathbf{a}_j$.

Table 3. *Interatomic bond distances (Å) for $PbO.2B_2O_3$*

Pb—O nearest neighbours			
Pb(1^{i})—O(2^{v,vi})	2.483 (5)	Sr(1)—O(1)*	2.63 (2)
Pb(1^{i})—O(1^{vii})	2.532 (7)	Sr(1)—O(2)*	2.52 (2)
Pb(1^{i})—O(3^{viii,ix})	2.664 (5)	Sr(1)—O(2)*	2.84 (2)
Pb(1^{i})—O(3^{iv,i})	2.894 (5)	Sr(1)—O(3)*	2.67 (1)
		Sr(1)—O(3)*	2.76 (1)
Pb—O second-nearest neighbours			
Pb(1^{i})—O(1^{vi})	3.010 (7)	Sr(1)—O(1)*	3.04 (2)
Pb(1^{i})—O(2^{iv,i})	3.020 (5)	Sr(1)—O(1)*	3.15 (2)
Pb(1^{i})—O(4^{x,xi})	3.105 (5)	Sr(1)—O(4)*	3.05 (1)
Pb(1^{i})—O(4^{i,iv})	3.158 (5)	Sr(1)—O(4)*	3.20 (1)
B—O tetrahedra			
B(1^{i})—O(3^{iii})	1.44 (2)	B(2^{i})—O(3^{iv})	1.411 (8)
B(1^{i})—O(2^{ii})	1.455 (9)	B(2^{i})—O(2^{ii})	1.434 (8)
B(1^{i})—O(1^{ii})	1.464 (8)	B(2^{i})—O(4^{xii})	1.550 (9)
B(1^{i})—O(4^{i})	1.56 (1)	B(2^{i})—O(4^{ii})	1.552 (9)

Symmetry codes: (i) x, y, z; (ii) $x - \frac{1}{2}, 1 - y, \frac{1}{2} - z$; (iii) $x - \frac{1}{2}, 1 - y, \frac{1}{2} + z$; (iv) $x, y, -z$; (v) $x - 1, y, z$; (vi) $x - 1, y, -z$; (vii) $x - 1, y - 1, z$; (viii) $x, y - 1, -z$; (ix) $x, y - 1, z$; (x) $x - \frac{1}{2}, -y, z - \frac{1}{2}$; (xi) $x - \frac{1}{2}, -y, \frac{1}{2} - z$; (xii) $x, y + 1, z$. * Sr—O bond distances are taken from Perloff & Block (1966), where atom labels, *e.g.* O(1), correspond to the same labels in the lead compound.

is that there is an oxygen, O(4), which is coordinated to three borons. The feature of three tetrahedra sharing one common oxygen is superimposed on Fig. 1 where a projection on (001) is shown.

This borate network leaves empty channels running along the [010] direction (Fig. 2) and it is here that the Pb ions are found. The Pb—O coordination is quite unclear as can be seen from Table 3. Using a cut-off value for the nearest neighbours of 3.0 Å, consistent with that used in $SrO.2B_2O_3$ (Perloff & Block, 1966), a coordination of seven is obtained compared with a coordination of nine obtained in $SrO.2B_2O_3$ using the same criteria. These seven bond distances vary from 2.483 (5) to 2.894 (5) Å, in which the 2.532 (7) Å bond distance is that of the single bond associated with O(1) being situated on a mirror plane at $z = 0$. The Pb atom is also on a special position, while the remaining atoms are all on general positions. The general atomic positions are: x, y, z; $x, y, -z$; $\frac{1}{2} + x, -y, \frac{1}{2} - z$; $\frac{1}{2} + x, -y, \frac{1}{2} + z$; and the special positions: $x, y, 0$ and $\frac{1}{2} + x, -y, \frac{1}{2}$.

5. Measurement of non-linearity

The experimental set-up used to estimate the optical non-linearity was based on the apparatus described by Kurtz & Perry (1968). Second-harmonic generation intensity data were obtained by placing a powder sample in an intense beam from a Q-switched Nd:YAG laser of wavelength 1064 nm. The output, filtered first to remove the fundamental wavelength, was then detected using a photomultiplier and displayed on an oscilloscope. This

procedure was then repeated using a standard non-linear material, in this case KDP (KH_2PO_4), and the ratio of the second-harmonic intensity outputs calculated. KDP samples were sieved to the particle size range 60–180 μm. Fig. 3 shows SHG intensity as a function of particle dimension for pure and barium-doped lead tetraborate. It is important to note that the intensity scale for the two materials in this diagram is not the same and that the intensities relating to the pure samples of lead tetraborate have been amplified for ease of viewing. The maximum intensity observed in any of the undoped samples was only around one quarter of the consistent intensity observed in the doped samples prepared with relatively large particle sizes. [Note that the barium-doped sample was prepared with 20Ba:80Pb, although later energy-dispersive X-ray analysis (EDAX), undertaken at Warwick University, revealed that the samples consisted of 30Ba:70Pb.]

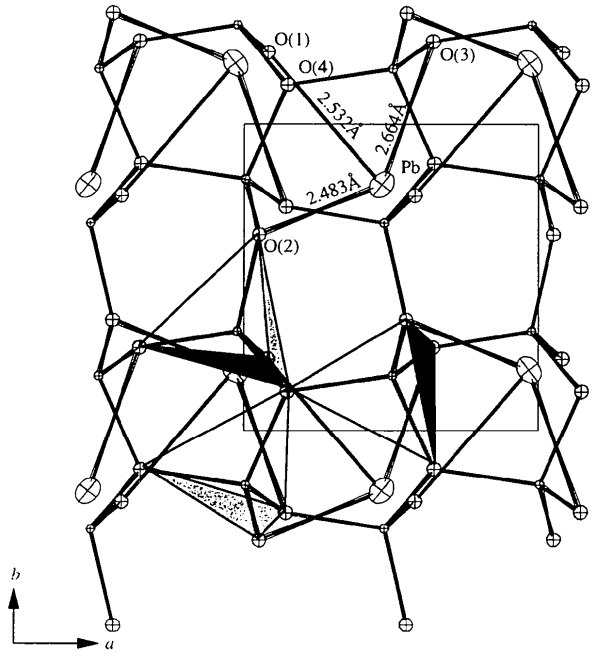

Fig. 1. A projection on (001) showing the five shortest Pb—O bonds and also the superimposed feature of three tetrahedra sharing a common oxygen.

Fig. 2 shows theoretical curves describing the variation of SHG efficiency with particle size observed in a Kurtz test for a non-phase-matching material, curve *A*, and a phase-matching material, curve *B*, of similar non-linearity. In a non-phase-matching material the maximum intensity is achieved when the particle size approximately matches the average coherence length and then falls with any increase in particle size. In a phase-matching material the intensity, in contrast, reaches a plateau at large particle sizes.

In Fig. 3 it is clear that for the pure lead tetraborate, the highest second-harmonic intensities are monitored in the samples prepared from small particle sizes, indicating that the material is non-phase-matchable. Although the intensity does not diminish consistently throughout the samples prepared with larger and larger particles, this is probably due to imperfect filtering allowing smaller particles to remain in the larger particle samples. The highest intensity recorded gave an estimated SHG efficiency of 8–16 times KDP (giving an

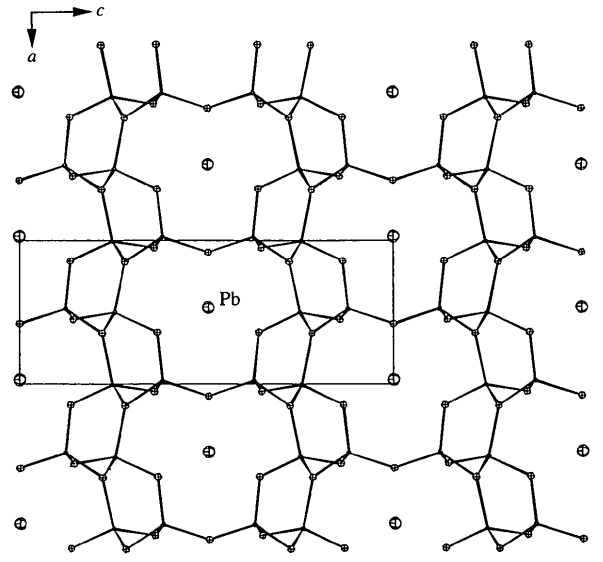

Fig. 2. A projection on (010) showing the tunnels left in the structure by the network of tetrahedra, where the Pb atoms are situated.

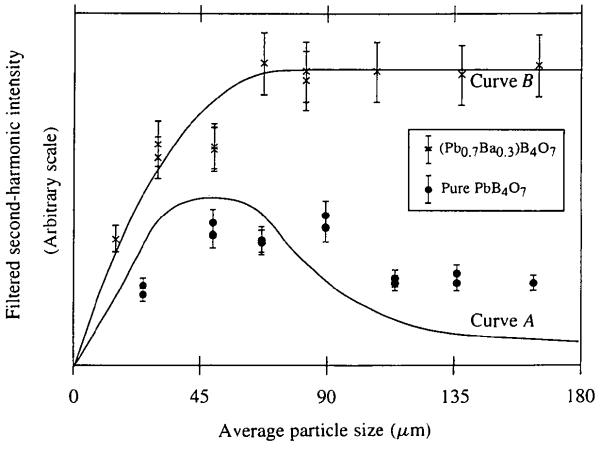

Fig. 3. The variation of SHG intensity with particle size for $PbO.2B_2O_3$ and $(Pb_{0.7}Ba_{0.3})O.2B_2O_3$ in the Kurtz and Perry test. The intensity units are not the same for the two materials as the $PbO.2B_2O_3$ measurements have been scaled up by a factor of approximately 2 for convenience. Theoretical curves are also presented which describe the basic features of the variation of SHG efficiency with particle size for a non-phase-matchable material, curve *A*, and a phase-matchable material, curve *B*.

estimated average effective non-linearity of around 3–4 times KDP). However, non-phase-matchability has a 'damping down effect' in this technique and, therefore, in such a case the true value of the average effective non-linearity could be significantly larger. Further support for this argument arises from the measurements taken on barium-doped lead tetraborate. Unlike with the undoped sample, a consistent second-harmonic intensity was measured throughout the samples containing larger particles, clearly indicating phase-matchability. The highest intensity recorded now gives an estimated SHG efficiency of 30–40 times greater than KDP and hence an estimated average effective non-linearity of around 5–6 times KDP.

6. Discussion

Considering the B—O network, we can see that there is a degree of distortion arising from the unusual occurrence of three tetrahedra sharing the same vertex. Although the presence of distorted anionic groups often indicates the possibility of a greater non-linearity, the contribution of the borate network to the optical non-linearity is still expected to be low simply because it comprises entirely the anions $(B_3O_9)^{9-}$, non-planar six-membered rings, connected by oxygen. These have been shown theoretically using the 'anionic group theory' method (Chen, Wu & Li, 1989) to possess very small NLO effects.

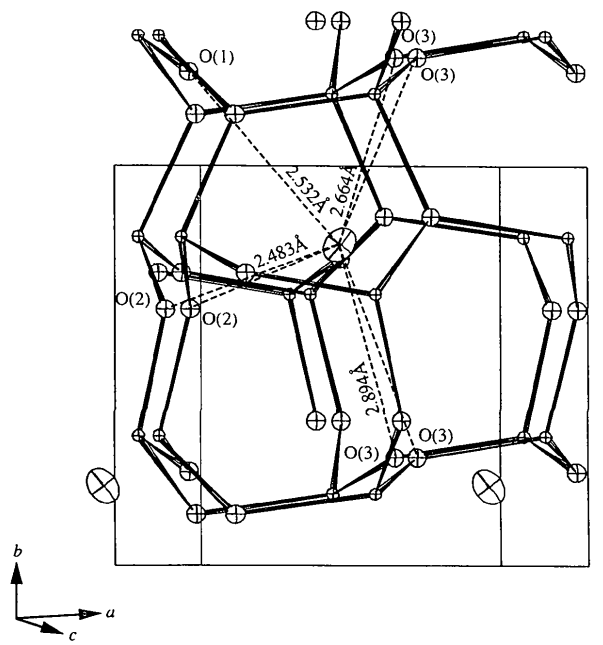

Fig. 4. A projection on (001) followed by a 5° rotation around the *y* axis, showing the first seven Pb—O bonds.

If we cannot attribute the considerable non-linearity shown by both sets of samples to the borate network, then we must assume that it originates in the Pb—O bonding. Certainly an aspect of the bonding which is clear is its asymmetry. If only the five shortest bonds are considered [2.483 (5)–2.664 (5) Å], it can be shown that all bonds lie to one side of the Pb atom, while the remaining two longer bonds [bond length 2.894 (5) Å] are to the opposite side. It is also worth pointing out that although the longest two bonds may reduce the overall non-linearity, their associated NLO bond polarizability 'β' will be smaller than those associated with the shorter bonds, hence reducing their destructive effect expected from (1). Similarly, the shortest Pb—O bond, *i.e.* Pb—O(2) of length 2.483 (5) Å, will have the largest NLO bond polarizability 'β' and hence is expected to hold the greatest contribution to the material's non-linearity and hence frequency-doubling capability.

It is this asymmetry of the shortest bonds, combined with the highly polarizable Pb atoms which is therefore expected to be the main contributor to the apparent high non-linearity. Fig. 1 shows only the first five shortest Pb—O bonds where the structure is projected on (001). Only three bonds can be seen owing to the mirror plane perpendicular to the *c* axis. However, the first five bonds can be clearly seen to lie to one side of the Pb. The position of the final two bonds can be seen in Fig. 4, where an enlarged projection on (001) followed by rotation of 5° about the *b* axis is shown.

Considering the relative polarizabilities of lead and barium, it seems reasonable to assume that the substitution of barium is unlikely to increase significantly the non-linear coefficients. Instead, the most obvious conclusion to the differences exhibited in the Kurtz test is that the barium simply increases the birefringence slightly, hence rendering the material phase-matchable and allowing the samples to exhibit an SHG efficiency truly representative of the average effective non-linearity of lead tetraborate. The reader is referred to Bismayer, Hensler, Salje & Güttler (1994) for an example of a study monitoring the change in birefringence induced by varying the Pb:Ba ratio in a solid solution. In conclusion, our work suggests that lead tetraborate doped with barium could be an important new NLO crystal.

DLC wishes to thank the Science and Engineering Research Council for a grant to enable this work to be carried out. We are also grateful to Mr S. York and Dr P. Thomas at the University of Warwick for performing the compositional analysis of the sample.

References

Bismayer, U., Hensler, J., Salje, E. & Güttler, B. (1994). *Phase Transit.* **48**, 149–168.

Chen, C., Wu, Y. & Li, R. (1989). *Int. Rev. Phys. Chem.* **8**, 65–91.

Hobden, M. V. (1967). *J. Appl. Phys.* **38**, 4365–4372.
Jeggo, C. R. (1971). DPhil. thesis, St Catherine's College, Oxford, England.
Kurtz, S. K. & Perry, T. T. (1968). *J. Appl. Phys.* **39**, 3798–3813.
Larson, A. C. (1970). *Crystallographic Computing*, edited by F. R. Ahmed, S. R. Hall & C. P. Huber, pp. 291–294. Copenhagen: Munksgaard.
Miller, R. C. (1964). *Appl. Phys. Lett.* **5**, 17–19.
Perloff, A. & Block, S. (1966). *Acta Cryst.* **20**, 274–279.
Prince, E. (1982). *Mathematical Techniques in Crystallography and Materials Science*. Berlin: Springer-Verlag.
Stoe & Cie (1985). *REDU4 Data Reduction Program*, *INDEX Automatic Indexing Program* and *DIF4 Data Collection Program*. Stoe & Cie, Darmstadt, Germany.
Watkin, D. J., Carruthers, J. R. & Betteridge, P. W. (1985). *CRYSTALS User Guide*. Chemical Crystallography Department, University of Oxford, England.